The Impact of RADARSAT ScanSAR Image Quality on Ocean Wind Retrieval

P.W. Vachon, J. Wolfe, R.K. Hawkins
Canada Centre for Remote Sensing
588 Booth St., Ottawa, Ont. K1A 0Y7 Canada
Phone: 613 995-1575 Fax: 613 947-1385
E-mail: paris.vachon@ccrs.nrcan.gc.ca
http://www.ccrs.nrcan.gc.ca

ABSTRACT

We compare image quality and radiometric calibration of several RADARSAT ScanSAR processors to assess impact on ocean wind retrieval. To address the relative state of ScanSAR processing, we arranged to have several ocean scenes processed by four different ScanSAR processors. We found some variability in image quality and radiometric calibration. Nevertheless, ScanSAR images should be able to provide useful high-resolution wind field information at near-synoptic scales.

INTRODUCTION

Ocean surface wind vector retrieval from ScanSAR images is a topic of emerging interest. For example, it has been shown that RADARSAT (C-band HH polarization) ScanSAR images could have a role in hurricane surveillance, polar low monitoring, and operational coastal wind field measurement. It is now well established that, knowing the radar geometry, the wind speed can be estimated from the SAR-observed radar cross section using a suitable wind retrieval model [6]. Hybrid C-band HH polarization models (consisting of a C-band VV polarization ERS scatterometer model such as CMOD_IFR2 and a suitable C-band polarization ratio) have been successfully demonstrated for use with single beam RADARSAT SAR images [8].

Unfortunately, the calibration of RADARSAT ScanSAR products has proven to be a rather long and difficult process. Complicating factors have included: our rather poor knowledge of the spacecraft's attitude leading to azimuth stripes due to errors in applied elevation antenna patterns; image scalloping that arises from errors in Doppler parameter estimation; the limited available dynamic range of ScanSAR image products; and the occurrence of analogue-to-digital converter (ADC) saturation.

The latter problem is now well understood. When ADC saturation occurs, a loss in signal power and a consequent underestimation of the radar cross section results. RADARSAT's automatic gain control (AGC) is essentially driven by only the contents of the near-half sub-swath [7]. Two acquisition strategies have been proposed to address this AGC problem. First, dynamic gain acquisitions can lead to saturation-induced dark bands over land and possible underflow over water. For this approach, it is recommended that the ocean target of interest be maintained in the near-half swath. Second, fixed gain acquisitions require an *a priori* decision by the user to supply a suitable gain setting. Of course, the appropriate gain for the ocean is wind speed dependent. For each strategy, the occurrence of saturation can be monitored in the signal data and calibration correction factors can be estimated by assuming a Gaussian signal data distribution.

We have obtained ScanSAR products from four RADARSAT processors: the Canadian Data Processing Facility (CDPF), the Tromsø Satellite Station (TSS), the Alaska SAR Facility (ASF), and *IOSAT*'s SentrySAR processor. In this paper, we present our understanding of the calibration status of these ScanSAR processors and we intercompare some derived data profiles. The comparisons are based on StormWatch data [2] acquired over a buoy near the Hibernia oil production platform (N46:45 W48:47) on the Grand Banks of Newfoundland during winter '97/'98 (Fig. 1), and a ScanSAR image of Hurricane *Danielle* (Fig. 2) acquired in August 1998 off the US East Coast, as summarized in Table 1. The high resolution (*i.e.*, 100's of meters) with which we can see the wind field's imprint on the ocean surface across the nearly 500 km swath of these images illustrates why RADARSAT ScanSAR images are of interest for high resolution (compared to scatterometry's 25 to 50 km resolution) wind field retrieval at near-synoptic scales.

CALIBRATION REQUIREMENT

We first consider the requirement on radiometric calibration for wind speed estimation from SAR images. In Fig. 3, we have plotted the wind speed error that would be expected for a given error in normalized radar cross section σ° at a particular incidence angle and for a known wind direction. From the plot, we see that in order to retrieve wind speeds to an accuracy of better

Table 1: Summary of ScanSAR data sets considered.

Data Set	Date/Time [UTC]	Pass	Wind
StormWatch	25-Nov-97 21:06	Asc.	18 m/s, 317°
StormWatch	19-Dec-97 21:06	Asc.	9 m/s, 304°
StormWatch	12-Jan-98 21:06	Asc.	n/a
StormWatch	01-Mar-98 21:06	Asc.	7 m/s, 19°
Danielle	31-Aug-98 10:51	Desc.	n/a

Table 2: Summary of ScanSAR processors considered.

Processor	Data Orientation	DN format	Output dynamic range control	ADC saturation compensation	Radiometric Calibration
CDPF	Zero Doppler	8-bit integer	output LUT, linear in β°	No	±1.35 dB (more for scallops) [5]
ASF	Beam Centre	8-bit integer	–25.5 dB to 0 dB, logarithmic in σ°	No	±0.2dB SCWB only [4]
TSS [3]	Beam Centre	8/16-bit integer	–30.1 dB to 22.5 dB, logarithmic in β°	Yes	No
SentrySAR	Beam Centre	8/16-bit integer or float	output LUT, linear in β°	Yes	Yes, error bar unknown

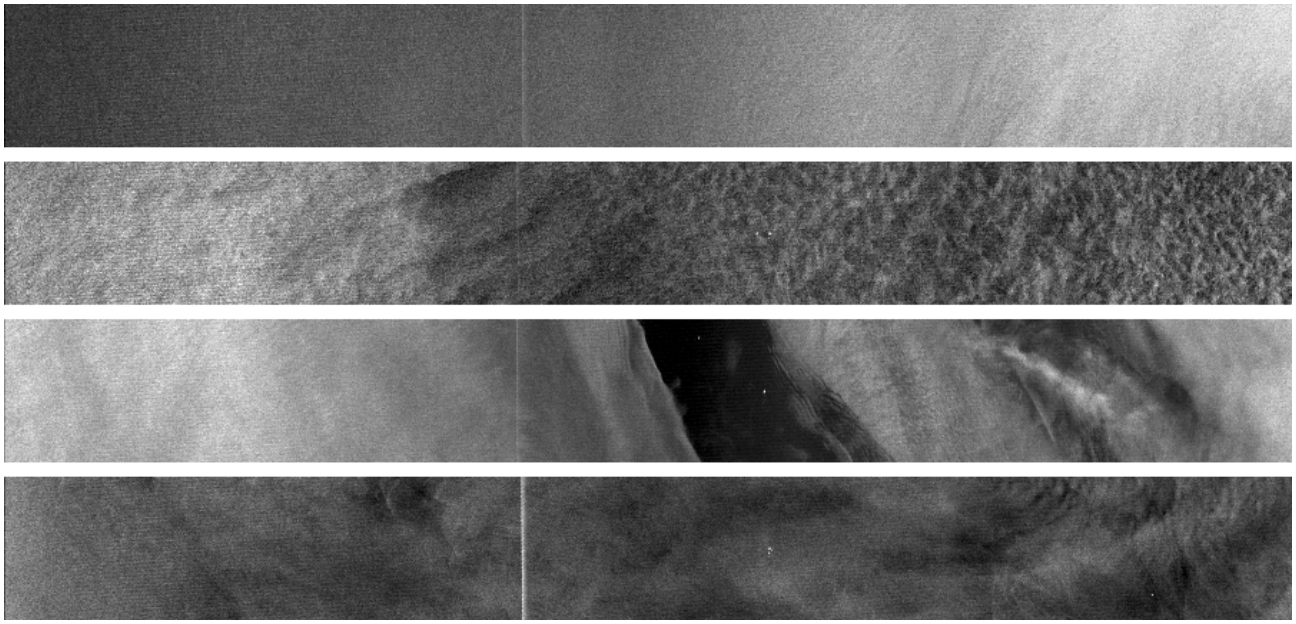

Fig. 1: RADARSAT ScanSAR Wide B images (CDPF) of Hibernia (right of centre) acquired during StormWatch: full swath, near edge to the left, sequenced as in Table 1. The line is nadir ambiguity. (CSA 1997 and 1998)

than 2 m/s, in general, we may need to achieve calibration that is much better than 1 dB, absolute, especially for the higher wind speeds that are of greater interest. This calibration tolerance assumes that the wind direction is known. The required tolerance on radar cross section is even smaller if the wind direction is also to be estimated from the SAR image since a wind direction error can also contribute to the error in the retrieved wind speed.

THE PROCESSORS

The salient details of the products from the available ScanSAR processors are summarized in Table 2. In each case, the SPECAN processing algorithm is used, so well known ScanSAR image quality problems, such as image scalloping, can arise in the event of errors in the estimated Doppler centroid. The image products are provided in varying geometries and with various radiometric calibration statuses, as noted. We only considered 8-bit image products. The TSS ScanSAR products are not radiometrically calibrated. For the TSS

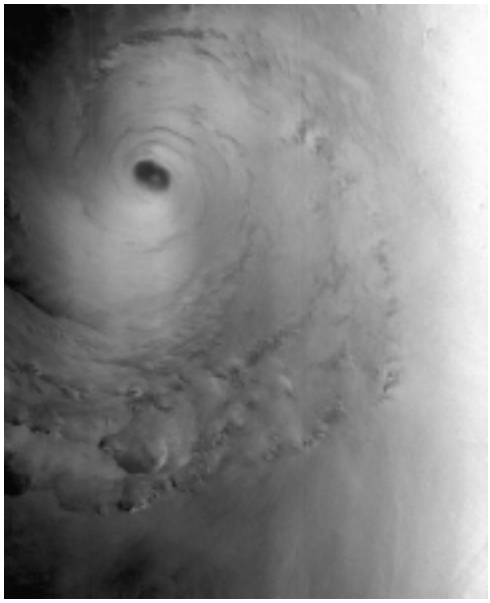

Fig. 2: RADARSAT ScanSAR Wide B image (SentrySAR) of Hurricane *Danielle*: full swath, near edge to the right. (©CSA 1998)

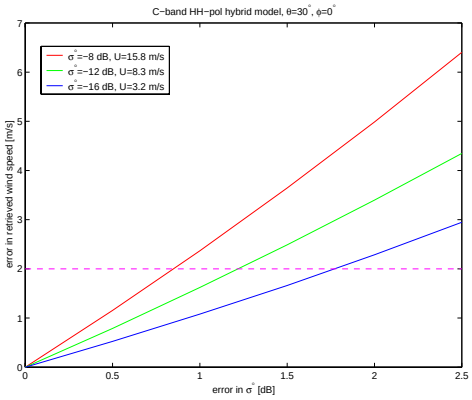

Fig. 3: Error in retrieved wind speed for a given error in σ° for a hybrid C-band HH polarization model at 30° incidence angle for the wind blowing towards the radar. We assumed that the wind direction is known.

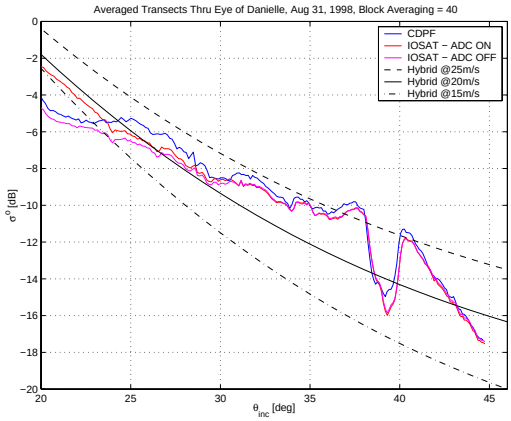

Fig. 4: σ° transect through the eye of Hurricane *Danielle* showing ADC saturation power loss compensation with the SentrySAR processor (labelled IOSAT – ADC on). The correction is important at the near edge of the scene.

products, we have subtracted 46 dB from the β° values interpreted from the digital numbers (DNs). While this is certainly not a robust calibration, this does serve to nominally align the TSS data with the data from other calibrated processors.

The TSS and SentrySAR processors can operationally carry out ADC saturation analysis and compensation. The impact of this correction for a fixed gain acquisition over a hurricane is illustrated by the radar cross section

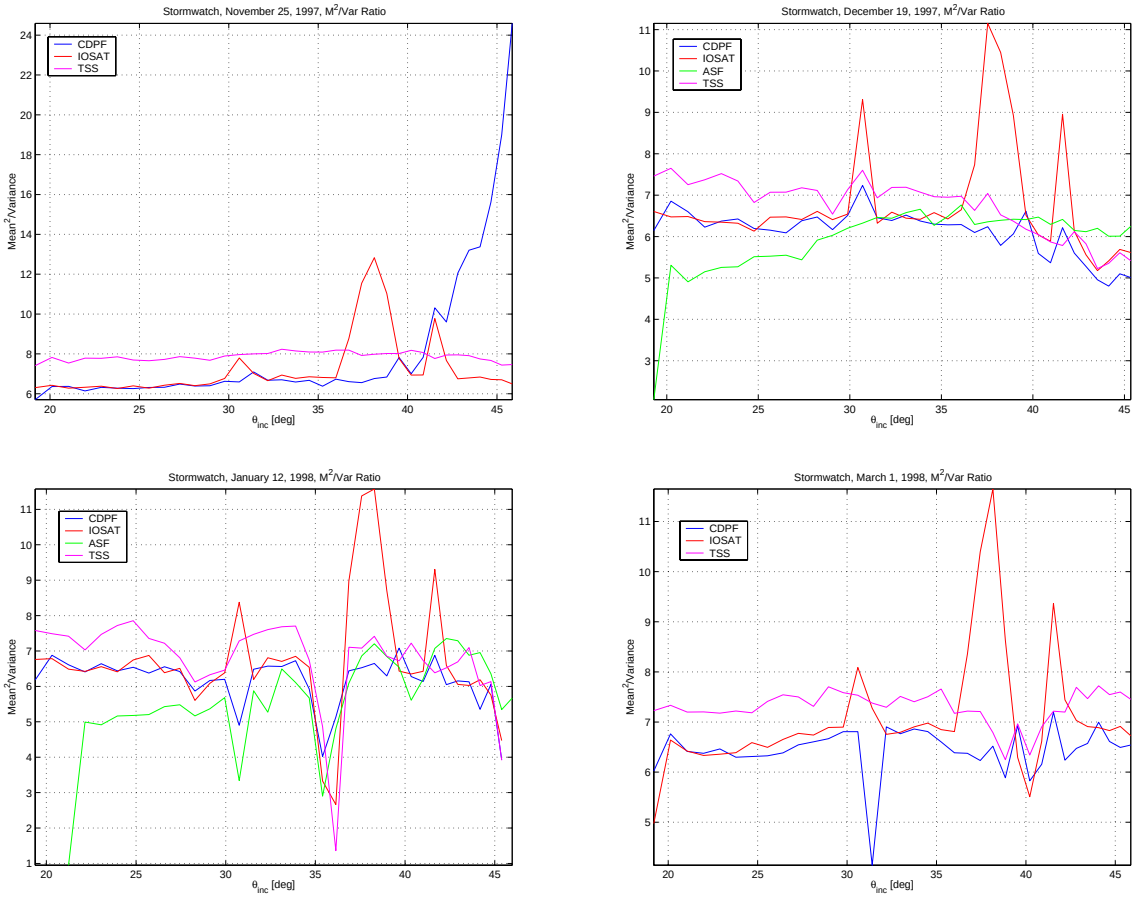

Fig. 5: MSVR as a function of local incidence angle for the StormWatch scenes, as available for each processor.

profiles shown in Fig. 4. The CDPF and ASF products tend to underestimate the radar cross section by up to 2 dB, especially for smaller incidence angles. In general, ADC saturation could arise for fixed gain acquisitions. It would become worse for higher wind speed situations, especially in the vicinity of the elevation antenna pattern maxima of each beam that makes up the ScanSAR image swath.

IMAGE QUALITY

As a check on image quality, we have inspected the images for obvious problems such as scalloping and inter-beam seams. Although these artifacts are not rare, none of the images that we worked with had dramatic problems in this regard. The worst case of scalloping was measured at about 0.7 dB peak-to-peak. The SentrySAR processor carries out platform orientation estimation in order to refine the Doppler centroid, and dynamically updates the orientation parameters within a scene [1]. The products from this processor had essentially immeasurable scalloping for the cases that we examined in this study.

As a quantitative check on image quality, we plotted the mean-squared-to-variance ratio (MSVR) as a function of local incidence angle through the Hibernia location for each of the StormWatch scenes (Fig. 5). We see that each processor has generated products with nominally 7 statistically independent looks. The local reduction in MSVR for all processors near 36° on Jan 12 is due to a local loss of the backscattered signal.

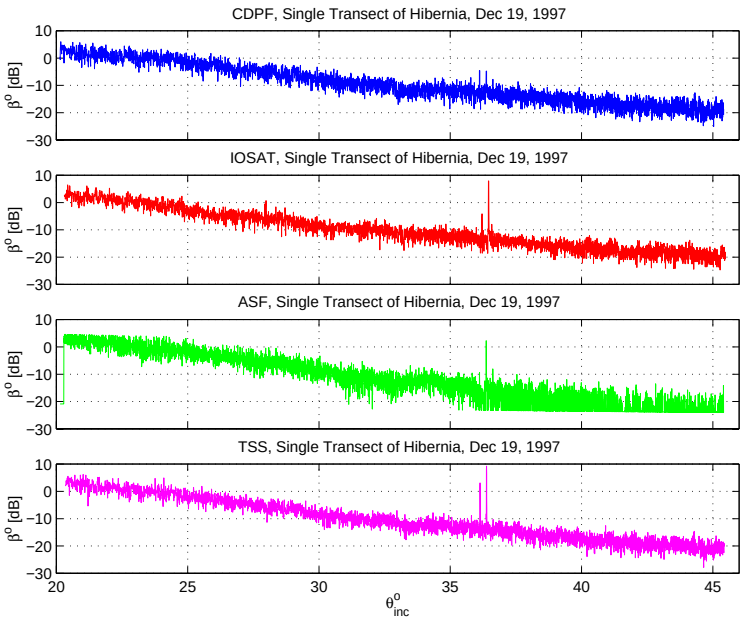

Fig. 6: A single transect of β° as a function of incidence angle for one StormWatch image.

The increase in MSVR at the far edge of the Nov. 25 CDPF product is attributed to overflow of the 8-bit DNs in the image product (*i.e.*, the output LUT was inappropriately large in this case). The ASF products show a roll-off in MSVR at the near edge. The reason for this is not so far understood.

For the SentrySAR products, and some of the others to a lesser extent, there is a local increase in MSVR in the vicinity of the interbeam seams. Presumably, this is caused by the SentrySAR blending the data in the entire beam overlap region, effectively increasing the local number of statistically independent looks. Furthermore, some of the processors show an increase in MSVR while others show a decrease in the vicinity of the W1 nadir ambiguity (near 31°, see the Jan. 12 transect, in particular). Again, we presume that the various processors treat the nadir ambiguity in different ways. The naidr ambiguity is most visible in the CDPF and ASF products. In Fig. 6 we show a single range β° transect for each processor through the Hibernia location. We see the effects of DN underflow and overflow, particularly for the ASF product. There is also some DN truncation for the CDPF product, but it is less obvious due to use of an output LUT to scale β° into an image DN.

RADIOMETRIC CALIBRATION

In Fig. 7, we show range transects of the mean normalized radar cross section σ° through the Hibernia location from each of the processors for which we have data available. The TSS and SentrySAR processors each used ADC saturation power loss compensation, although these scenes were actually acquired using dynamic gain.

We have also plotted, for reference, some model transects of radar cross section based upon a hybrid C-band HH polarization wind scatterometry model that is composed of CMOD_IFR2 and a polarization ratio based on Kirchhoff scattering [8]. The central model curve is based on the *in situ* measured wind vector that is assumed to apply across the entire swath (except for the 12 Jan. '98 case, for which an *in situ* wind vector was not available). The other two model curves correspond to the measured wind speed plus or minus 2 m/s. If the

radiometric calibration is satisfactory, we would expect that the SAR-observed radar cross section profiles should agree with the model in the vicinity of the Hibernia platform (near 36° local incidence angle), while the slope of observed profiles should agree with the model slope, at least in the vicinity of the wind vector measurement.

We see that, in general, the transects from the various processors agree with each other to within several dB. The exception is that the ASF data show smaller radar cross sections, compared to the other processors for the two available cases, at least for larger incidence angles. We also see reasonable agreement with the model curves, particularly in the vicinity of the *in situ* measurement. The variability in radar cross section as a function of incidence angle is a measure of the variability in local wind speed across the nearly 500 km image swath. However, radar cross section discrepancies at these scales suggest that the calibration of certain of these processors is not accurate enough to support wind field estimation to within 2 m/s. At this point, we do not know which processor has provided data with the best calibration.

For completeness, in Fig. 8 we show a normalized radar cross section transect in azimuth through one of the StormWatch scenes. We do not see any systematic differences among the available data sets in the azimuth direction, aside from the smaller radar cross sections from the ASF product that were noted earlier.

CONCLUSIONS

We have compared RADARSAT ScanSAR ocean images processed on 4 different ScanSAR processors with the ocean wind retrieval application in mind. In general, we found comparable image quality among the processors. The occurrence of inter-beam seams and the degree of scalloping tended to be small for these open ocean images. Such images do not have large backscatter changes over small distances in azimuth, making Doppler centroid estimation straightforward.

In some cases, underflow and overflow of the digital numbers in the image products caused problems with

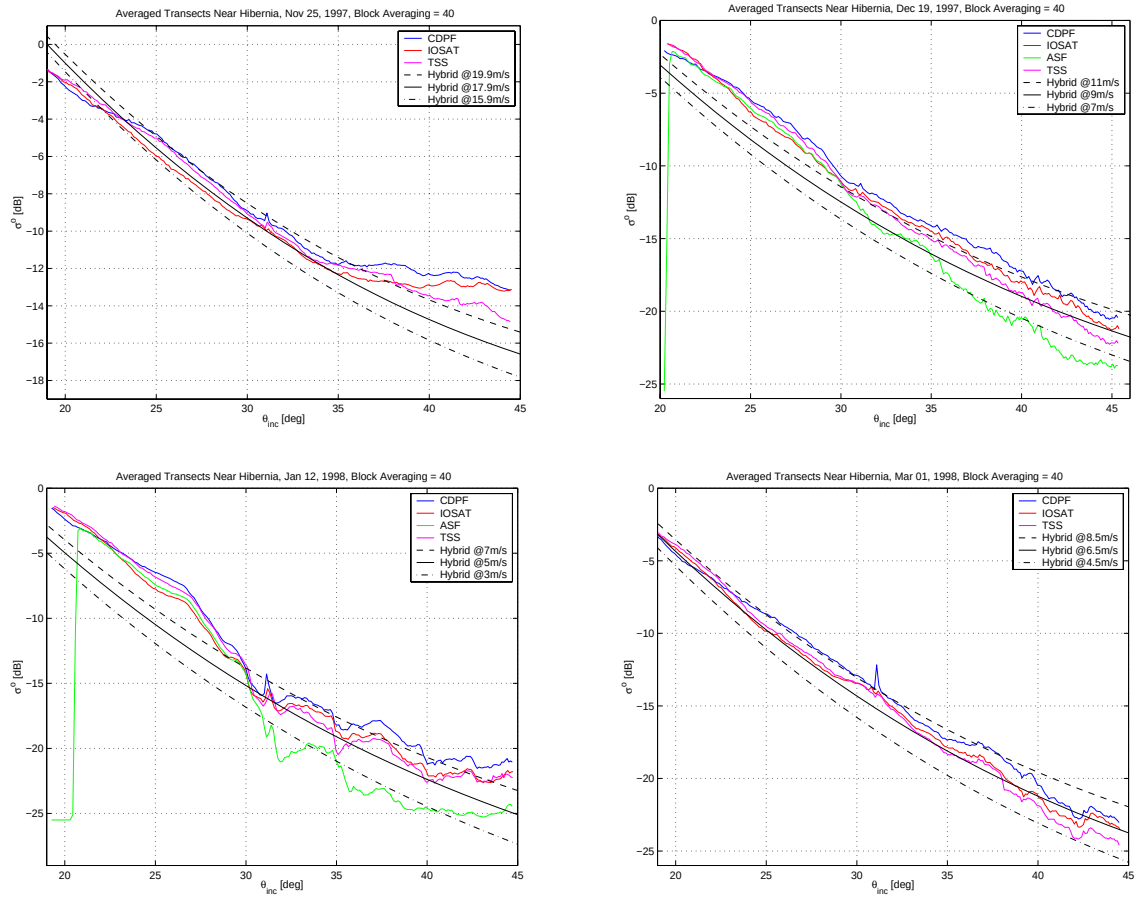

Fig. 7: σ° as a function of local incidence angle for the StormWatch scenes, as available for each processor. Also plotted are hybrid C-band HH polarization model cross sections for the wind speed and direction (if available) measured at Hibernia and that speed ± 2 m/s.

image quality and calibration. Digital number overflow can be a problem for higher wind speeds.

Each processor had a similar MSVR for open ocean regions with measurable backscattered power, in spite of differences in the way the DNs are coded and scaled in the image products. Evidently, some of the processors treat the beam overlap region in different ways.

ADC saturation power loss could be a problem under some circumstances. It is recommended that a correction based on signal data saturation analysis is applied routinely to all images. This satuation problem becomes more severe for larger wind speeds if the image was acquired with a fixed gain. Unfortunately, there may be little evidence in the image for this saturation, and the product does not provide information on the gain settings that were actually used.

The radiometric calibration agreed to within several dB among the processors considered. Exceptions were when ADC saturation power loss occurred and was not compensated, and the ASF products that indicated lower radar cross sections at larger incidence angles.

It appears that the radiometric calibration of RADARSAT ScanSAR images could support the ocean wind retrieval application. The caveats are that the raw digital numbers in the images should be examined for overflow, ADC saturation power loss, if present, should be compensated, and that radiometric problems could arise locally if image scalloping occurs. However, at this point, further analysis is required to understand the noted discrepancies in normalized radar cross section. Analysis of Amazon rainforest and (adequately sampled) calibration transponder images could provide new insight in this regard.

ACKNOWLEDGEMENTS

We thank Tony Bauna (TSS) and Marina Dragošević (IOSAT) for helpful discussion, supplying image products and information on their processors, and for their interest in this project. The ASF data were obtained through PWV's participation in the Alaska SAR Facility User Working Group (ASFUWG). Fred Dobson (BIO) supplied the Hibernia wind measurements.

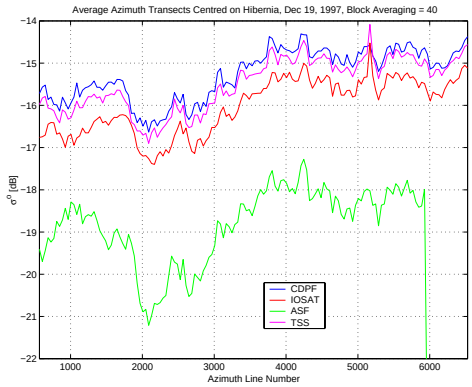

Fig. 8: σ° as a function of azimuth position for the various processors, as available, for one of the StormWatch scenes.

REFERENCES

[1] Dragošević, M.V., "On accuracy of attitude estimation and Doppler tracking", these proceedings.

[2] http://fermi.jhuapl.edu/sar/stormwatch/index.html

[3] Kongsberg Spacetec, "MEOS, SAR Satellite Instrument Processor, Product Description", SIP-PD-SPT-SY-0001, 8 October 1999

[4] Martyn, P., *et al*., "Calibration of the RADARSAT SWB processor at the Alaska SAR Facility", Proc. IGARSS'99, 28 June to 2 July 1999, Hamburg, Germany.

[5] Srivastava, S.K., *et al*., "Maintaining image quality and calibration of RADARSAT-1 CDPF products", Proc. IGARSS'99, 28 June to 2 July 1999, Hamburg, Germany.

[6] Vachon, P.W., and F.W. Dobson, "Validation of wind vector retrieval from ERS-1 SAR images over the ocean", *The Global Atmosphere and Ocean System*, Vol. 5, pp 177-187, 1996.

[7] Vachon, P.W., *et al*., "Adaptive compensation of RADARSAT SAR analogue-to-digital converter saturation power loss", Geomatics in the ERA of RADARSAT (GER'97), CD-ROM Proceedings, 27-30 May 1997, Ottawa, Ont., Canada.

[8] Vachon, P.W., and F.W. Dobson, "Wind retrieval from RADARSAT SAR images: Selection of a suitable C-band HH polarization wind retrieval model", to appear, *Can. J. Rem. Sens.*, 2000.